Pure & Appl. Chem., Vol 56, No. 12, pp 1715-1726, 1984.
Printed in Great Britain.

0033-4545/84 $3.00 + 0.00
Pergamon Press Ltd.

IN SITU STUDIES OF THE HIGH TEMPERATURE OXIDATION OF METALS AND ALLOYS

Robert A. Rapp

Department of Metallurgical Engineering, The Ohio State University,
Columbus, Ohio, 43210, USA

Abstract - *In situ* observations of the oxidation of pure metals which form cation-diffusing scales have been made in a hot-stage environmental scanning electron microscope (HSESEM). Some common features and many differences were observed for the growth of oxide scales on pure copper, iron, nickel and chromium. The formation of non-planar scale morphologies (whiskers, pyramids and pits) originates from the role of screw dislocations in providing ledges for lattice extension at the scale/gas interface. Questions remain concerning the exact nature and origin of these dislocations and the atomistic steps occurring at the metal/scale interface.

INTRODUCTION

The study of scale growth on pure metals has been a popular research topic for fifty years since the publication of Wagner's classic theoretical paper describing parabolic scale growth (1). Investigations of the high temperature oxidation of metals such as copper, iron, nickel and chromium which grow cation-diffusing scales, and which form the bases for many important engineering alloys, have received particular attention. At sufficiently high temperatures ($T \gtrsim 0.75T_{melt}$ for the scale), parabolic scaling constants for the oxidation or sulfidation of metals forming cation-diffusing scales generally agree with those calculated from Wagner's theory (1,2) using electrical conductivity or self-diffusion data for the scale compound. This agreement supports the validity of the principal assumptions of the theory: local equilibrium at both the gas/scale and metal/scale interfaces, and independent rate-limiting migration of ions and electrons (holes) through the lattice of the single-phase scale layer which is not affected by morphological imperfections such as grain boundaries, dislocations, fissures, or voids.

At intermediate scaling temperatures ($0.5T_m \lesssim T \lesssim 0.75T_m$), scale growth on metals deviates from Wagner's ideal parabolic behavior. Single crystal spheres of iron (3), copper and nickel (4) exhibit different scale textures and morphologies resulting in differing scaling rates on the various crystallographic faces. Herchl, Khoi, Homma and Smeltzer (5) oxidized nickel single crystals with (100), (111), and (110) faces at 500 to 800°C and reported differing "effective" (best fit) parabolic scaling rate constants. These rate constants and those for polycrystalline nickel (6) are higher and their activation energies are lower than those values extrapolated from higher temperatures where lattice diffusion is rate limiting. In fact, Herchl et al. (5) show that scale growth on nickel single-crystal faces is not really parabolic, but rather the instantaneous parabolic constant generally decreases with time, correlating to an increase in scale grain size resulting from grain growth. For the oxidation at 500°C in P_{O_2} = 0.5 torr of three copper single crystals with differing minor deviations from the (001) face, Matsunaga and Homma (7) reported differing oxidation kinetics resulting from a shift in the frequency of four equivalent epitaxial grains, and therefore the corresponding grain boundaries.

In a series of self-diffusion and scaling kinetics measurements for nickel and iron at intermediate temperatures, Atkinson et al. (8-12) showed that the growth of NiO and Fe_3O_4 is consistent with scale growth rate control by grain boundary diffusion. This conclusion—rate control by grain boundary diffusion at intermediate scaling temperatures—is generally accepted in the literature today, and semi-empirical theories (7,13) have found reasonable correspondence to the experimental results.

Tentatively accepting this model for cation transport, one must still inquire about the mechanism for lattice extension during scale growth at the scale/gas interface. The

traditional kink-ledge-terrace (KLT) model for crystalline surface structure shown in Fig. 1 is familiar to many other areas of surface science, but has found little application in

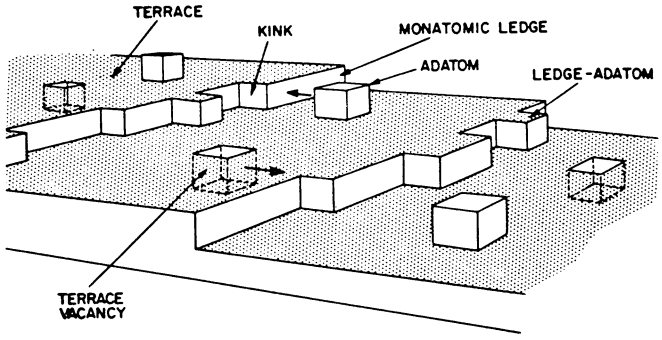

Fig. 1. Schematic idealized atomic model for structure of surface close to low-index plane.

rationalizing the evolution of surface morphology for scaling reactions. With this intended goal, and realizing the interesting complication that the cation flux may arrive to the surface by predominant grain boundary diffusion, we have studied the evolution of scale morphology in the growth of cation-diffusing scales in a hot-stage environmental scanning electron microscope (HSESEM).

IN SITU STUDIES OF OXIDE SCALE GROWTH

The details of the HSESEM have been reported previously (14) and some results have been published (15-18). The oxidizing gas is introduced to the SEM vacuum through a 1mm ID Pt tube, and an equivalent pressure is reported as that pressure providing the same collision frequency with the surface. A few example results will be presented here to illustrate commonalty and differences in the scaling behavior of the pure metals Cu, Fe, Ni and Cr.

Copper Oxidation (16)

The oxidation of OHFC, electropolished copper heated to 930°C in vacuum resulted in the morphology sequence shown in Fig. 2. The heating of copper in vacuum provided a tenacious initial oxide film which resulted in a retarded nucleation rate but an exaggerated rapid cuprous oxide grain growth at later times. This rapid growth of flat featureless grains seen in Fig. 2 was driven by growth stresses, as capillarity effects could not be important. At sufficiently high temperatures (T > 850°C) the micrographs show an illuminated phase at the oxide grain boundaries in the HSESEM. As explained recently (16,17), this effect results from a slight surface coverage by a Cu_2O fume which is formed by gas-phase collisions between evaporated copper atoms and the incident O_2 flux. Thus, fume formation in oxidation occurs only when the vapor pressure of copper is significant, and the effect is also somewhat specific to the environment of the HSESEM.

On certain rather rare occasions, the growth of Cu_2O at high temperatures would result in the generation of an obvious fissure (surface void) in an oxide grain boundary after several hours oxidation; such a fissure would quickly fill with oxide fume. This phenomenon is consistent with the dissociation model for the formation of a porous internal scale (19) whereby the vacancy annihilation required for cation diffusion occurs preferentially along scale boundaries. While the observation of grain boundary fissures is not unexpected, and is especially well documented for metal sulfidation (20), the relatively rare incidence of obvious fissures is perplexing. Grain boundary fissures have been observed for relatively stationary boundaries, but not those experiencing rapid grain growth.

Pure copper heated in hydrogen and oxidized at 900°C in $P_{O_2} = 10^{-4}$atm formed small prismatic (pyramidal) Cu_2O grains. The rapid nucleation and impingement of these Cu_2O grains, which did not rapidly coarsen or flatten, minimized fume formation. Cold working the initial surface by shot peening increased the nucleation frequency and decreased the oxide grain size (16).

At lower intermediate temperatures (500°C) small pyramidal grains with relatively flat surfaces were formed, and occasionally a spiral macroledge was seen on the surface. In the

intermediate temperature range, scale growth was not observed to be localized at scale grain boundaries (no grain boundary ridges), but rather the lattice was apparently extended at surface ledges maintained by screw dislocations intersecting the surface. At intermediate and lower temperatures, copper oxide (probably CuO) whiskers were observed to grow or be reduced (in vacuum) at their tips; whisker growth was especially stimulated by trace H_2O in the O_2 gas, and by prior surface deformation.

Summarizing for copper oxidation, flat Cu_2O scales are seldom observed, and the more usual pyramidal grains (even at high temperatures) do not grow preferentially at grain boundaries. The specific oxide morphology observed depends upon temperature, experimental procedure and environment, surface deformation, and perhaps other factors (metal purity, etc.).

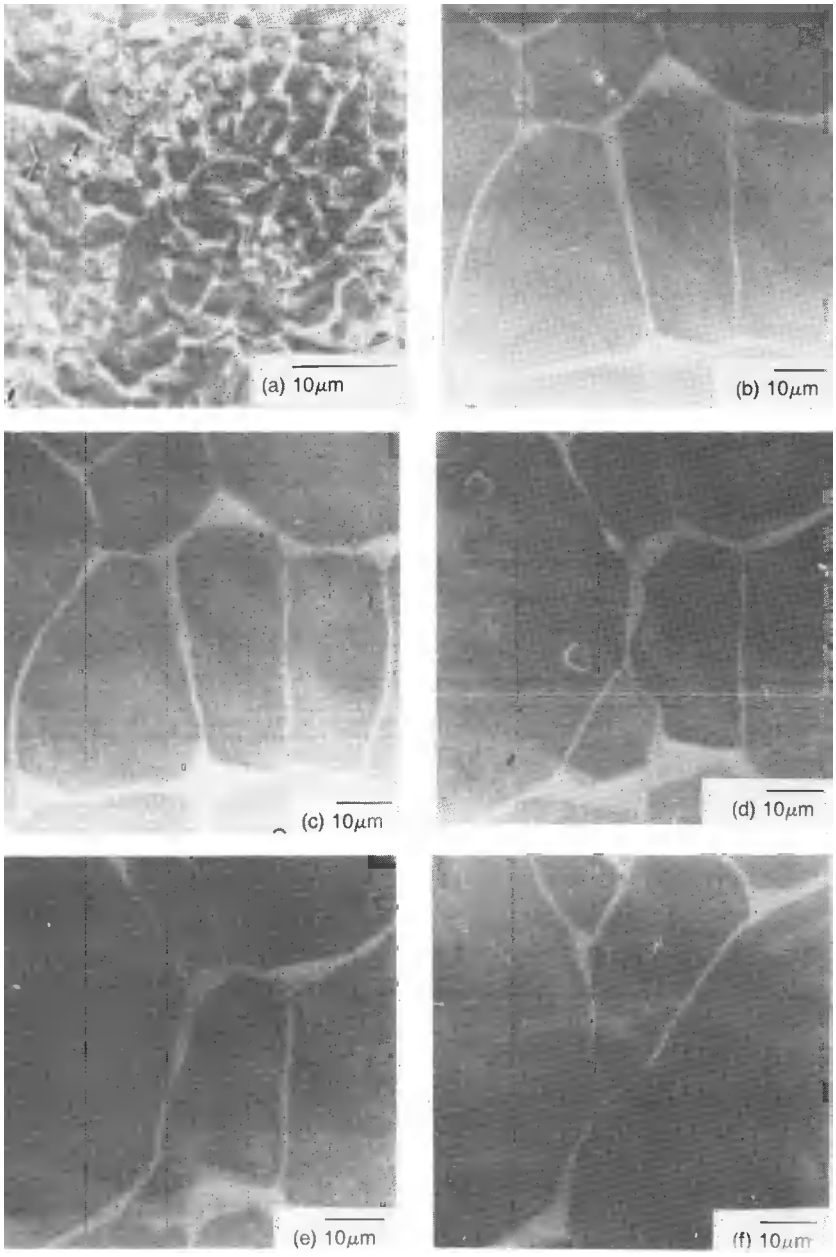

Fig. 2. Oxide scale formed on OFHC copper at 930°C in P_{O_2} = $3x10^{-4}$atm in HSESEM after (a) 30 s (2000X), (b) 195 min (1000X), (c) 210 min, (d) 242 min, (e) 244 min, (f) 271 min. (16)

Iron Oxidation (21)

The oxidation of very pure iron in the HSESEM at the very high temperature of 1200°C resulted in the growth of wustite (for several hours before Fe_3O_4 nucleation) exhibiting growth pits as a dominant feature. Figure 3 shows a sequence of in situ micrographs of wustite growth from a videotape over a period of 75 seconds. Pits are seen to evolve ledges from the pit nadir and macroledges are seen to traverse the oxide terraces resulting in crystal growth. The growth pits in wustite have $\{110\}$ faces which exhibit macro- and microfacets of $\{100\}$ planes. The growth pits are clearly centered on a dislocation intersection at the surface, and are probably maintained by a minimization of surface energy and dislocation line tension. The limited rate of oxygen arrival for $P_{O_2} \tilde{<} 10^{-4}$atm precludes local equilibrium

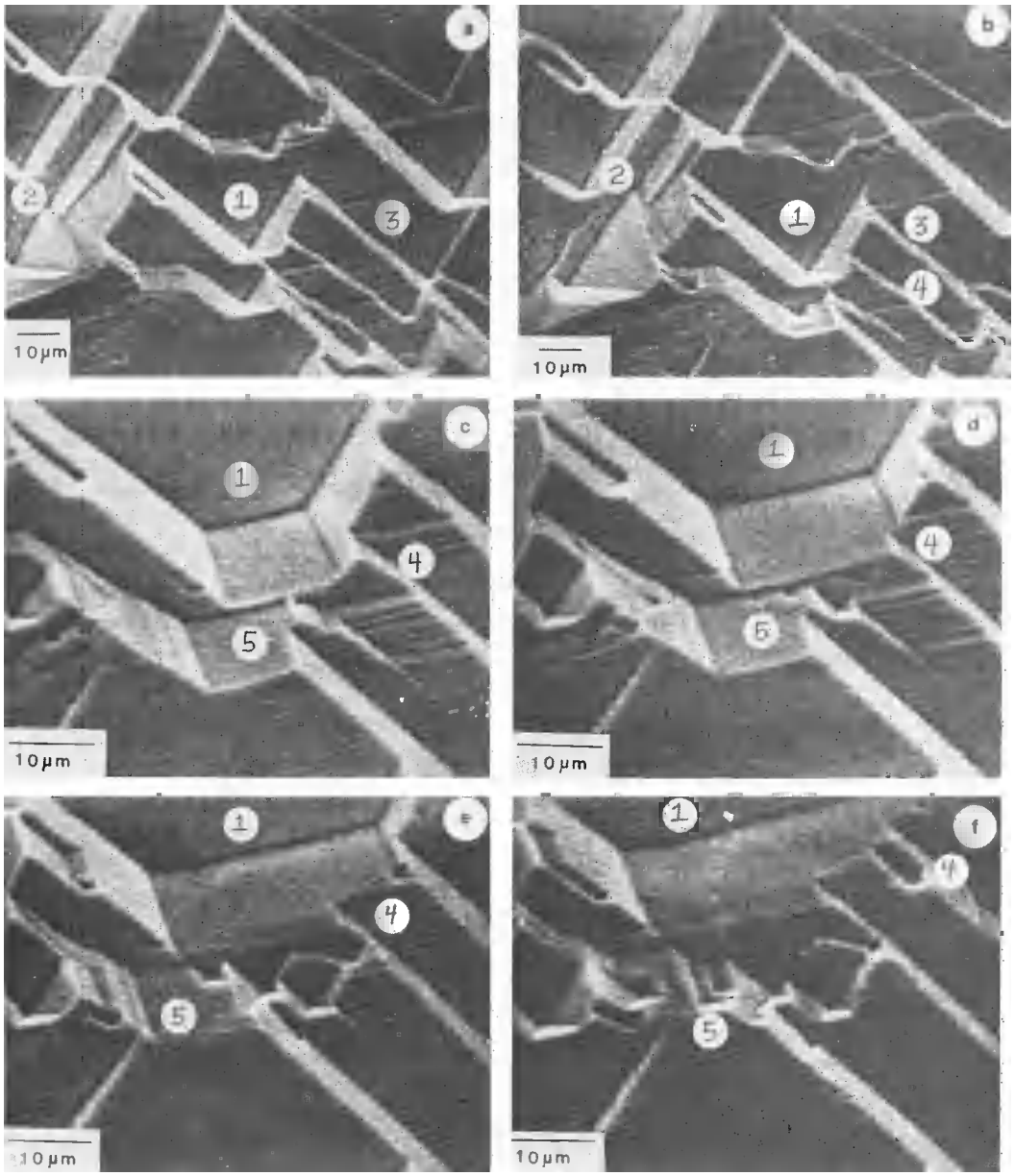

Fig. 3. Sequence of in-situ micrographs from videotape showing behavior of growth pits and surface ledges for growth of wustite on Fe at 1200°C in HSESEM for $P_{O_2} \tilde{<} 10^{-4}$atm: (a) zero time, 1000X, (b) 20 s, 1000X, (c) 40 s, 2000X, (d) 53 s, 2000X, (e) 65 s, 2000X (f) 75 s, 2000X

of the wustite surface with the oxygen, and thereby permits enhanced surface migration for cations required to maintain pits. As seen in Fig. 3, the pits exhibit active (sharp nadir)/inactive (flattening of the base) cycles which is consistent with the model suggested in Fig. 4 where edge jogs are shown in the screw dislocation responsible for pit growth. The climb of the edge jog to intersect the surface would offset the intersection such that the pit would flatten out for some period until the base of the pit was again intersected by the screw dislocation. Then the pit would be reactivated off-center, and a macroledge would transverse the face of the pit and contribute to scale growth. These specific features are consistent with the active/inactive/active pit behavior seen in Fig. 3 and in similar experiments.

The exact nature and origin of the dislocation responsible for pit growth are subjects of continuing research. From an experiment similar to that shown in Fig. 3, a wustite scale of about 100 μm thickness with wustite grain diameter of about 100-200 μm was tightly adherent to the iron substrate, but was spalled upon immersion in liquid nitrogen. Figure 5 shows montages of the external surface and the oxide at the scale/metal surface. A heavily pitted columnar wustite grain exhibited about $3x10^5$ pits/cm^2, and the corresponding oxide surface at the metal/scale interface exhibited protruding oxide nodules of density about $7x10^5$ nodules/cm^2. For the case of tightly adherent columnar scales, the origin of the dislocations in the oxide may be the underlying metal substrate. Hexagonal growth pits have been observed when a columnar Cr_5S_6 scale is grown on pure Cr or Fe-66Cr alloy at a very reduced P_{S_2} and and high temperature (22). Although these scales were detached from the metal, again a reasonable correspondence in density between surface pits and nodules (pyramids) at the scale/metal interface was found.

At low temperatures (450-500°C) α-Fe_2O_3 blades or platelets are grown, especially in the presence of water vapor. The metal transport required for whisker growth has been ascribed to cation diffusion along either a planar twin interface (23) or a hollow central core or pipe in the whisker (24) consistent with the presence of a screw dislocation with large Burgers vector (25).

Nickel Oxidation (26)

The growth of NiO scale on pure Ni has also been observed in the HSESEM. At very high temperatures (1350°C), pits or slotted pits are observed as shown in Fig. 6. The explanation for pit formation would parallel that suggested previously for wustite growth, but because of the slow cation diffusion in NiO, higher temperatures are required to avoid local equilibrium at the oxide/gas interface.

Figure 7 shows the faceted, pyramidal NiO grains formed upon the oxidation of H_2-heated (cold worked) Ni wire at 1000°C. Although NiO growth is believed to be supported by grain boundary diffusion at 1000°C, oxide growth clearly does not occur at these boundaries which exhibit deep crevices and incomplete closure at the surface. Indeed, transport by cation surface diffusion from the metal along oxide grain surfaces would seem more consistent with the scale morphology. For such NiO scales and those grown at lower temperatures, the nucleation of new grains can be observed *in situ* at the scale/gas interface. Any coarsening of the scale morphology is extremely slow. Figure 8 shows that stubby NiO whiskers are grown in dried O_2 at 1000°C, but the introduction of water vapor results in an immediate rapid growth of hair-like NiO whiskers. For all of the metals studied, filamentary whisker growth is tied to the presence of H_2O vapor.

The *in situ* observation of scale morphologies for Cu, Fe and Ni have led to the qualitative model for scale growth illustrated schematically in Fig. 9. At relatively low temperatures, surface cation diffusion up the hollow core (pipe) of a whisker can provide a relatively high cation flux to the whisker tip. With rate-limiting O_2 arrival or dissociation at the whisker tip for oxidation in pure O_2, the cations would percolate out the tip and down the outside surface before they are incorporated into the lattice to thicken the whisker. However, in the presence of H_2O vapor, the H_2O dissociation step should be much faster than that for O_2 such that the cations would contribute to lattice extension locally near the tip, and thin filamentary whiskers would be grown. For intermediate temperatures, a similar screw dislocation may provide the ledges required for lattice growth, but grain boundary diffusion for cations in series with surface diffusion should provide the cation flux, so that pyramidal crystals are grown. At very high temperatures, at least when the oxidant arrival rate is limited so that significant cation surface diffusion is possible, the screw dislocation intersections stabilize growth pits; the cation flux would be provided by lattice diffusion.

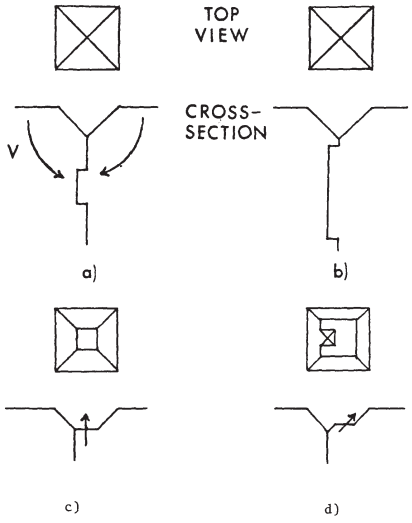

Fig. 4. Influence of edge jogs on dislocation pit behavior: (a) and (b) edge jogs climbs as a result of vacancy annihilation, (c) edge jog temporarily removes the dislocation from the pit nadir, (d) dislocation reactivates pit; macroledge traverses pit face.

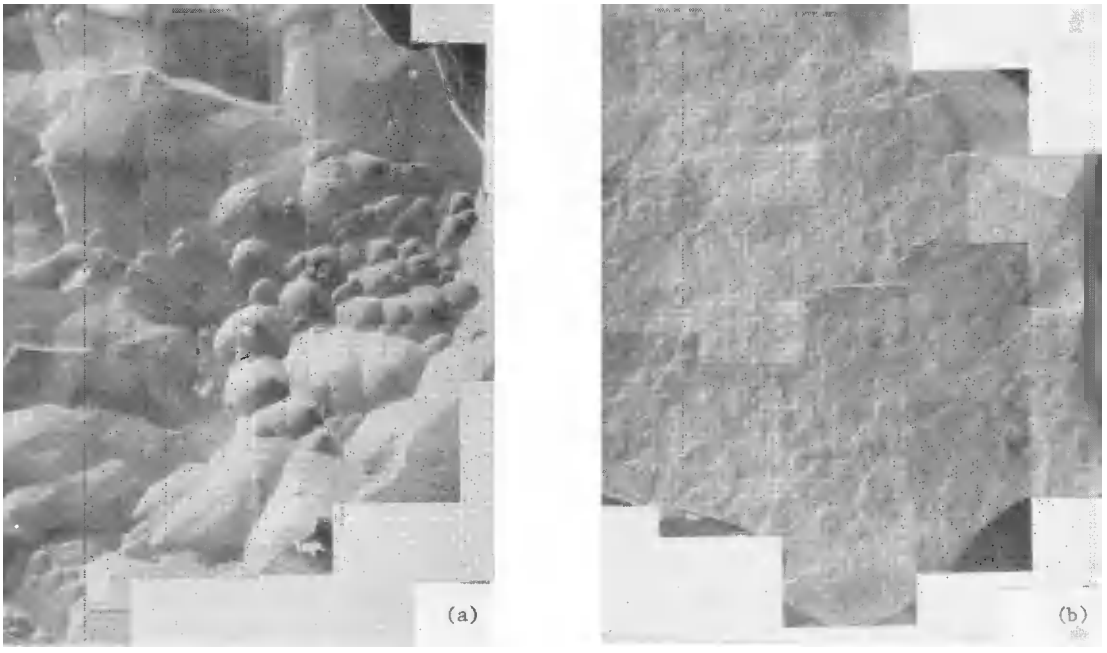

Fig. 5. Montages showing pit morphology at wustite/O_2 interface (a) and corresponding oxide nodules at wustite/iron interface (b) 375X before reduction. (10 μm markers are shown)

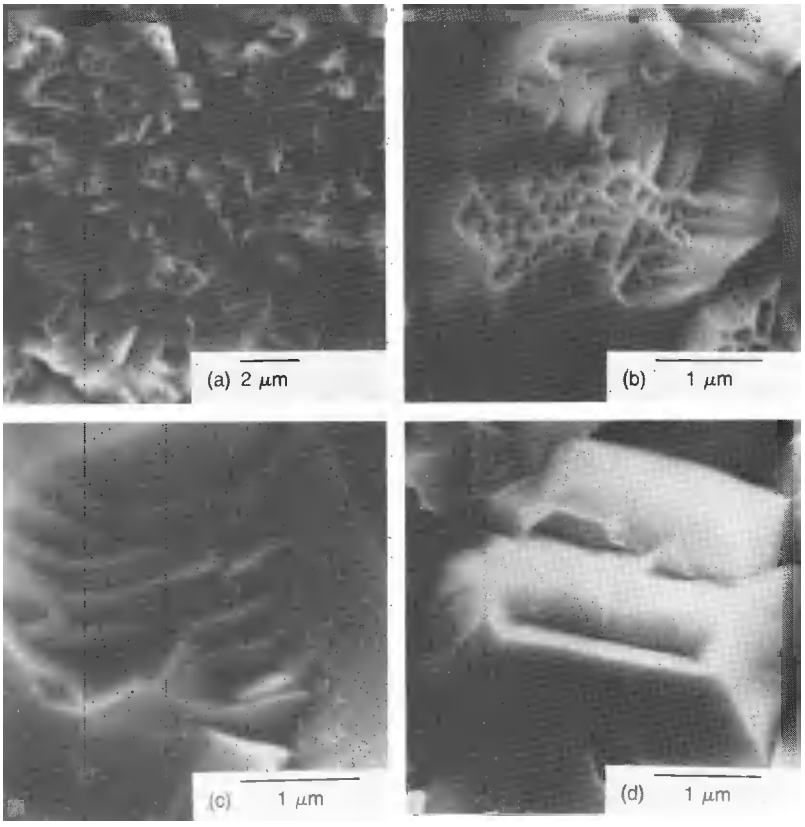

Fig. 6. Morphologies of NiO scale/gas interface after oxidation of 99.999% Ni in $P_{O_2} = 3x10^{-4}$atm at 1350°C for 15 min (a) 5,000X, (b) 23,000X, (c) 23,000X, (d) 18,000X. Examined in SEM at room temperature following oxidation.

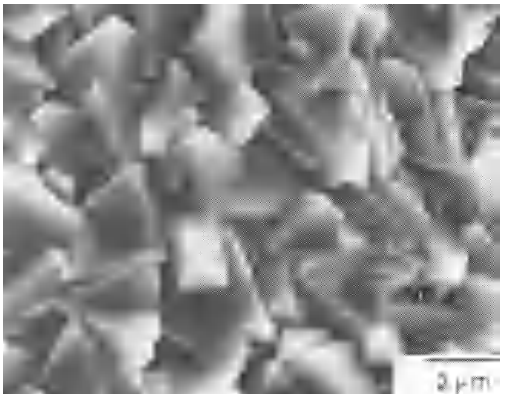

Fig. 7. Morphology of NiO scale/gas interface after oxidation of 99.99% Ni wire at 1000°C in $P_{O_2} = 3x10^{-4}$atm (dried) after 2 h 7 min (7000X). Examined in SEM at room temperature following oxidation.

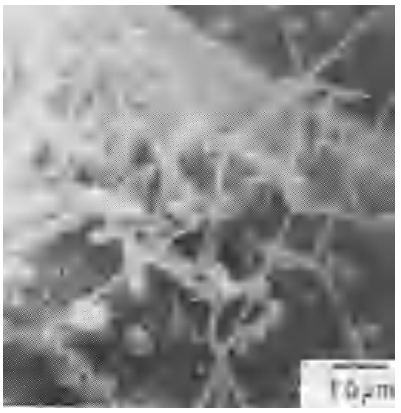

Fig. 8. In situ morphology of NiO scale/gas interface after oxidation of 99.99 pct Ni wire at 1000°C in $P_{O_2} = 3 \times 10^{-4}$ atm (dried) for 1 h 45 min followed by 5 min exposure to water vapor addition to O_2. Magnification 1000 times.

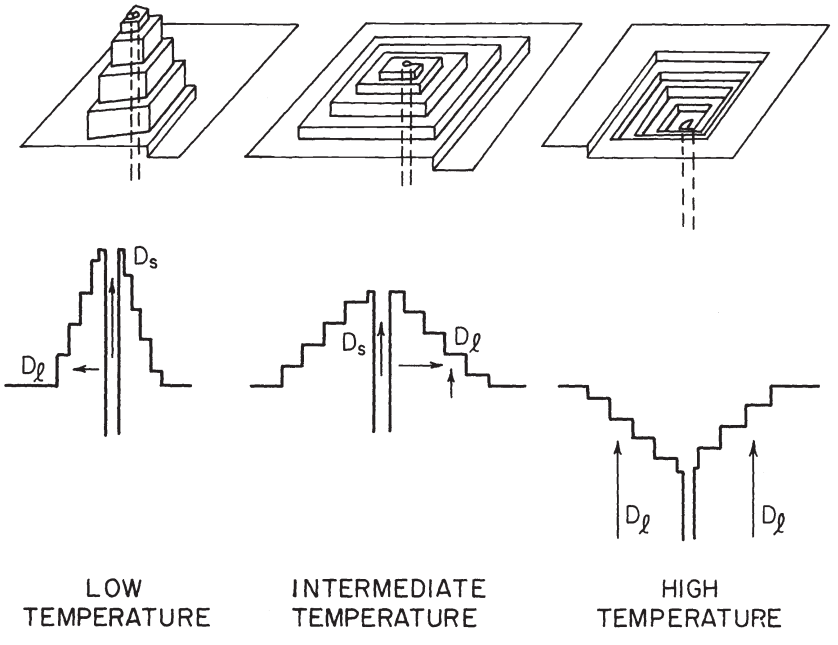

Fig. 9. Schematic illustration of role of dislocations in scale growth at low, intermediate, and high temperatures (26).

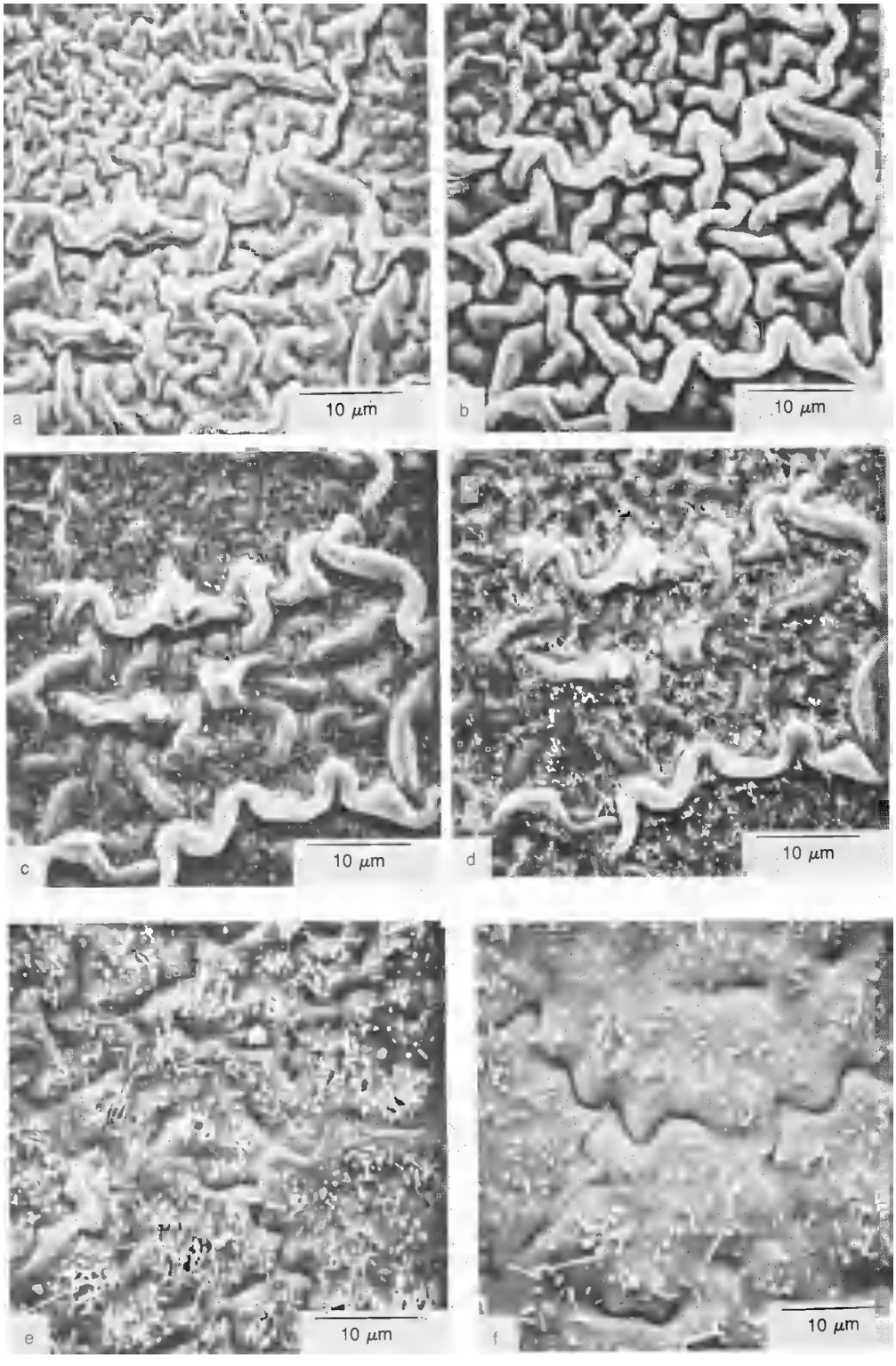

Fig. 10. HSESEM micrographs of electropolished and chemically etched arc-melted Cr that was heated in H_2 to 1100°C and subsequently oxidized at 1100°C and $P_{O_2} \tilde{>} 3x10^{-4}$atm for various times. (a) In H_2 at 1100°C, (b) to (h) in O_2 for various times: (b) 1.5 min, (c) 7 min, (d) 12 min, (e) 45 min, (f) 1 h 14 min. Magnification 2000 times.

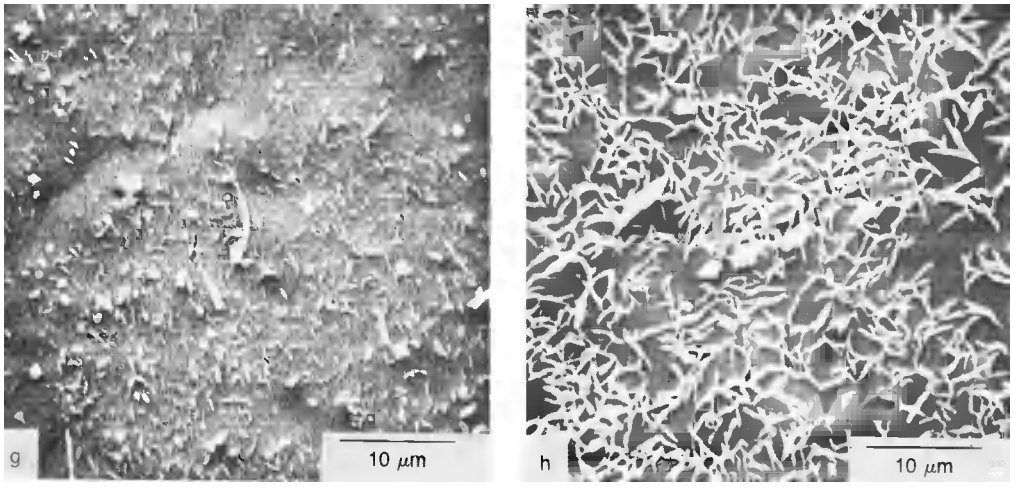

Fig. 10. (Continued)—HSESEM micrographs of electropolished and chemically etched arc-melted Cr that was heated in H_2 to 1100°C and subsequently oxidized at 1100°C and $P_{O_2} \approx 3 \times 10^{-4}$ atm for various times. (g) 2 h 2.5 min, and (h) 5 h 21 min. Magnification 2000 times.

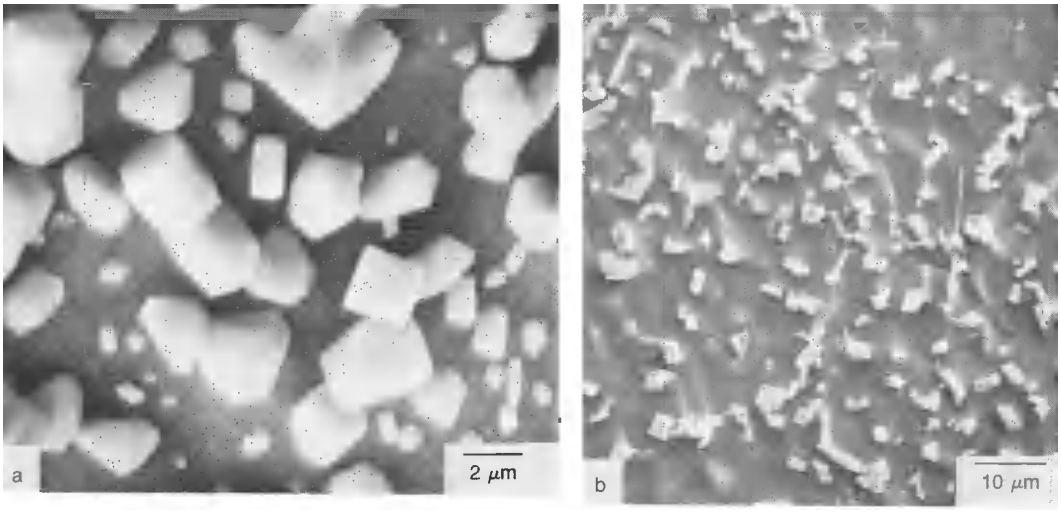

Fig. 11. Post-oxidation SEM micrographs of the oxide scale and the reacted Cr surface after oxidation at 1100°C in $P_{O_2} \approx 3 \times 10^{-4}$ atm for 6 h. (a) Scale surface facing the metal, (b) reacted Cr surface from which the scale has detached. Magnification of (a) 4250 times and of (b) 1020 times.

Chromium Oxidation (27)

Previous studies (28,29) of the oxidation of pure Cr have shown special morphological features different from those for Cu, Fe and Ni. Figure 10 shows the evolution of Cr_2O_3 scale morphology upon the oxidation of arc-melted pure Cr heated in H_2 to 1100°C and exposed to $P_{O_2} \tilde{<} 3x10^{-4}$atm in the HSESEM. Even in the H_2 beam, the initial oxidation of Cr and formation of the familiar scale convolutions could not be avoided (Fig. 11a). During exposure to oxygen in the special HSESEM environment of reduced total pressure, the convolutions are seen to shrink by evaporation and finally disappear. It is well known that the cation transport for scale growth is supplied for grain boundary diffusion via Cr evaporation across the gap separating the convolution from the underlying metal. In Figs. 10c-h, Cr_2O_3 whiskers are seen to grow between the convolutions where attachment to the metal is maintained, but not on the convolutions. After some extended period of oxidation, the convolutions have evaporated (Fig. 10h), and the surface is covered with whiskers. Thus, the formation of convolutions is not necessarily a steady-state feature of Cr_2O_3 growth, and can be avoided in several ways, including the use of dispersed oxides or reactive additions in the alloy (18). Upon post-oxidation spallation of the Cr_2O_3 scale shown in Fig. 10, large prismatic crystals (presumably Cr_2O_3) are found in the Cr/Cr_2O_3 interface as the only points of attachment. Because the density of these crystals (Fig. 11b) approximates that for the Cr_2O_3 whiskers at the scale/gas interface, again a causal relationship is suggested (18).

Oxide convolutions are also found in the growth of Al_2O_3 on Al-containing alloys, where again the Al vapor pressure is sufficient to provide the metal flux across the boundary. However, Al_2O_3 scales are thought to grow inward by oxygen grain boundary diffusion. For Al_2O_3 scales, tightly adherent areas do not develop whiskers, but they are grown on the detached, convoluted scale (30). This behavior is opposite to that for Cr_2O_3 growth and is not understood. Also for poorly adherent Al_2O_3 scales, large prismatic Al_2O_3 crystals serve as attachment points across the scale/gas interface (31). These observations must ultimately provide a better understanding for the growth mechanisms for Cr_2O_3 and Al_2O_3 scales.

CONCLUSIONS

In situ observations of oxide scale growth at the scale/gas interface in the HSESEM have provided some insights concerning mechanisms for lattice extension. However, the particular HSESEM environment also introduces certain features (fume formation, scale evaporation) which are specific to the experimental conditions (intermediate oxidant and total pressures). Such studies are ideally suited to examine the effects of sudden changes in the gas composition or temperature, and such studies are in progress. As known from the literature, many of the morphological and transport characteristics of scaling reactions depend upon many factors: specimen purity and preparation, oxidation procedure, temperature and the environment. Thus, scaling models must include qualifying and restrictive limitations.

ACKNOWLEDGEMENTS

For their experimental and interpretative contributions to these HSESEM studies, I wish to thank: G. M. Raynaud, J. P. Hirth, S. K. Verma, H. Erhart, S. K. Bose, T. L. Jungling, and M. Lee. The research was supported by the Division of Materials Sciences, Office of Basic Energy Sciences, Department of Energy, on Contract DE-AC-02-79ER10404, and an Exxon Fellowship.

REFERENCES

1. C. Wagner, Z. phys. Chem. B21, 25-41 (1933).
2. C. Wagner, in Atom Movements, p. 153, ASM, Metals Park, Ohio (1951).
3. J. B. Wagner, K. R. Lawless, and A. T. Gwathmey, Trans. Met. Soc. AIME 221, 256-261 (1961).
4. J. V. Cathcart, in Oxidation of Metals and Alloys, D. L. Douglass, ed., p. 17, ASM, Metals Park, Ohio (1971).
5. R. Herchel, N. N. Khoi, T. Homma, and W. W. Smeltzer, Oxid. Metals 4, 35-49 (1972).
6. D. Caplan, M. J. Graham, and M. Cohen, J. Electrochem. Soc. 119, 1205-1215 (1972).
7. S. Matsunaga and T. Homma, Oxid. Metals 10, 361-376 (1976).
8. A. Atkinson and R. I. Taylor, J. Materials Sci. 13, 427-432 (1978).
9. A. Atkinson, R. I. Taylor, and P. D. Goode, Oxid. Metals 13, 519-543 (1979).

REFERENCES (Continued)

10. A. Atkinson and R. I. Taylor, Phil. Mag. A. 39, 581-595 (1979). ibid. 43, 979-998 (1981).
11. A. Atkinson, R. I. Taylor, and A. E. Hughes, in High Temperature Corrosion, R. A. Rapp, ed., P. 110, NACE, Houston, TX (1983).
12. A. Atkinson, M. L. O'Dwyer, and R. I. Taylor, J. Materials Sci. 18, 2371-2379 (1983).
13. J. M. Perrow, W. W. Smeltzer, and J. D. Embury, Acta Metall. 16, 1209-1218 (1968).
14. S. K. Verma, G. M. Raynaud, and R. A. Rapp, Oxid. Metals 15, 471-483 (1981).
15. S. K. Verma, G. M. Raynaud, and R. A. Rapp, in Chemical Metallurgy, A Tribute to Carl Wagner, N. A. Gokcen, ed., p. 419, TMS-AIME, Warrendale, PA (1981).
16. G. M. Raynaud, W.A.T. Clark, and R. A. Rapp, Metall. Trans. 15A, 573-586 (1984).
17. G. M. Raynaud and R. A. Rapp, Metall. Trans. 15A, 587-593 (1984).
18. R. A. Rapp, Metall. Trans. 15A, 765-778.
19. A. Dravnicks and H. McDonald, J. Electrochem. Soc. 94, 139 (1948).
20. S. Mrowec and T. Werber, Gas Corrosion of Metals, p. 87, Foreign Scientific Publ., Warsaw (1978).
21. T. L. Jungling and R. A. Rapp: "High Temperature Oxidation of Iron at 1200°C in a Hot-Stage Environmental Scanning Electron Microscope," accepted for publication in Metall. Trans A. 1984.
22. T. Narita, W. W. Smeltzer, and K. Nishida, Oxid. Metals 17, 299-314 (1982).
23. R. L. Tallman and E. A. Gulbransen, J. Electrochem. Soc. 115, 770-775 (1968).
24. D. A. Voss, E. P. Butler, and T. E. Mitchell, Metall. Trans. A. 13A, 929-935 (1982).
25. F. C. Frank, Acta Cryst. 4, 497-501 (1951).
26. G. M. Raynaud and R. A. Rapp: "In Situ Observation of Whiskers, Pyramids and Pits During the High Temperature Oxidation of Metals," Proceedings of International Metallographic Society Meeting, Calgary, July 1983.
27. S. K. Bose, H. Erhart, and R. A. Rapp, unpublished research.
28. D. Caplan and G. I. Sproule, Oxid. Metals 9, 459-472 (1975).
29. P. Kofstad and K. P. Lillerud, J. Electrochem. Soc. 127, 2397-2410 and 2410-2419, (1980); Oxid. Metals 17, 177-194 and 195-203 (1982).
30. J. K. Tien and F. S. Pettit, Metall. Trans. 3, 1587-1599 (1972).
31. S. Guruswamy, J. P. Hirth, and G. W. Powell, Oxid. Metals 19, 77-98 (1983).